

Large-Amplitude Dynamic Analysis of Composite Moderately Thick Elliptical Plates

M. Sathyamoorthy*

Clarkson University, Potsdam, New York

This paper is concerned with the study of large-amplitude flexural vibration of clamped, moderately thick composite elliptical plates. Von Kármán-type field equations, which are given in terms of the three displacement components of the plate, are used in this work. Included in these field equations are the effects of transverse shear deformation and rotatory inertia, such that they can readily be used for moderately thick plates of any plate geometry. Solutions to these governing equations are obtained by using a multiple-mode approach and employing Galerkin's method and the numerical Runge-Kutta procedure. Of the three nonlinear governing equations, exact solutions are reported for two. Based on these solutions, numerical results are reported for different types of high-modulus fiber-reinforced elliptical plates. Present results indicate significant influences of transverse shear deformation, modal interaction, material, and plate parameters on the nonlinear static and dynamic behavior. For both static and dynamic cases, present results are in excellent agreement with all those available in the literature for the special cases of thin plates.

Nomenclature

a	= semimajor axis
b	= semiminor axis
$A(\tau), B(\tau)$	= amplitude functions
$E_{\xi}, E_{\eta}, G_{\xi\eta}, \nu_{\xi\eta}, \nu_{\eta\xi}$	= material constants
h	= thickness of plate
$N_{\xi\xi}, N_{\eta\eta}, N_{\xi\eta}$	= stress resultants
$q(\xi, \eta)$	= lateral load
q_0	= uniformly distributed lateral load
q_0^*	= nondimensional load
R_i	= tracing constant for rotatory inertia
r	= aspect ratio, a/b
t	= time
T_s	= tracing constant for transverse shear
u^0, v^0, w^0	= displacement components
w_0^*	= nondimensional deflection or amplitude (w_{\max}/h)
x, y	= coordinate system
ξ, η	= nondimensional coordinates
ρ	= mass density
τ	= nondimensional time
β	= thickness parameter, a/h
ω	= nonlinear frequency including transverse shear and rotatory inertia
ω_0	= linear frequency without transverse shear and rotatory inertia
$\epsilon_1^0, \epsilon_2^0, \gamma$	= median surface strains

Introduction

LARGE-AMPLITUDE vibrations of thin plates of various geometries have been studied by several researchers.^{1,2} Most of the investigations reported so far make use of the widely known von Kármán theory extended to dynamic problems by Herrmann.³ Plates with various in-plane boundary

conditions have been treated using this theory. For thin plates with immovable-type in-plane boundary conditions, a simple Berger-type approximation based on the neglect of the second invariant of the middle surface strains in the expression for the extensional strain energy was used. In the case of elliptical plates, solutions to large-amplitude vibration problems have been reported by Sathyamoorthy and Chia^{4,5} using von Kármán-type nonlinear equations and by Banerjee⁶ using Berger-type simplified nonlinear governing equations. It must be pointed out here that the dynamic governing equations based on these theories do not take into account the effects of transverse shear deformation and rotatory inertia, which are very important in the study of moderately thick plates.⁷

Several nonlinear plate theories that take into account the effects of transverse shear deformation and rotatory inertia have been reported in the literature. A theory that was based on Berger approximation was used by Wu and Vinson⁸ to find solutions to moderately thick orthotropic rectangular plates. The limitation of the Berger approximation is that it could be used only for plates with immovable in-plane boundary conditions. Using the finite element method, Kanaka Raju and Venkateswara Rao⁹ studied the effects of transverse shear deformation and rotatory inertia on the large-amplitude vibration behavior of isotropic circular plates. Some recent investigations by the author^{7,10} are based on an improved nonlinear vibration theory that is an extension of the dynamic von Kármán plate theory applicable for thin plates. Equations corresponding to this theory have been derived using tracing constants that identify the effects of transverse shear deformation and rotatory inertia. When the tracing constants are dropped from these equations, the nonlinear dynamic equations corresponding to the thin-plate theory are readily obtained. Based on this theory, results are reported in the literature for plates of various geometries and boundary conditions. Most of these results are obtained assuming a single-mode approximation for the lateral mode.

In this paper, the nonlinear static as well as dynamic analysis of composite plates of elliptical geometry is reported. The nonlinearities investigated here are due to large-deflection or large-amplitude vibration and are appropriately included in the strain-displacement relations. Assuming the stress-strain relationship to be linear, the governing equations that account for the effects of transverse shear deformation and rotatory inertia are

Received Feb. 4, 1985; presented as Paper 85-0653 at the AIAA/ASME/ASCE/AHS 26th Structures, Structural Dynamics and Materials Conference, Orlando, FL, April 15-17, 1985; revision received March 19, 1986. Copyright © American Institute of Aeronautics and Astronautics, Inc., 1985. All rights reserved.

*Associate Professor, Department of Mechanical and Industrial Engineering.

presented in terms of the three in-plane displacement components u^0 , v^0 , and w of the plate. With the aid of a polynomial multiple-mode function for w , solutions to the three dynamic equations are obtained so as to satisfy all the in- and out-of-plane boundary conditions exactly. It is interesting to note that such a procedure leads to exact solutions for the in-plane displacements u^0 and v^0 . The expressions for the lateral displacement w and the in-plane displacements u^0 and v^0 are then used to solve the nonlinear equations representing the motion of the plate in the lateral direction. This solution procedure finally results in a set of nonlinear time-differential equations that are in terms of the amplitude functions found in the lateral displacement w . The Runge-Kutta method has been used to find numerical solutions to these modal equations.

Results are presented in this paper for certain high-modulus composites as well as isotropic elliptical plates with clamped immovable boundary conditions. Numerical results in terms of the variation of nonlinear frequencies with the amplitude of vibration are presented for some of the material and geometric parameters of the elliptical plate. The effect of coupling the vibration modes is discussed, along with a comparison of the current results with those of a single-mode approach. Results applicable for thin plates are also presented. For all the special cases, the present results are in close agreement with those found in the literature.

Governing Equations

The geometry of the plate and the coordinate system are shown in Fig. 1. For a rectilinearly orthotropic elliptical plate of uniform thickness h , semimajor axis a , and semiminor axis b , the governing von Kármán-type nonlinear dynamic equations are^{7,10}

$$au^0_{,\zeta\zeta} + p^2 r^2 au^0_{,\eta\eta} + s^2 rav^0_{,\zeta\eta} = -w_{,\zeta}(w_{,\zeta\zeta} + p^2 r^2 w_{,\eta\eta}) - s^2 r^2 w_{,\eta} w_{,\zeta\eta} \quad (1)$$

$$k^2 r^2 av^0_{,\eta\eta} + p^2 av^0_{,\zeta\zeta} + s^2 rau^0_{,\zeta\eta} = -rw_{,\eta}(k^2 r^2 w_{,\eta\eta} + p^2 w_{,\zeta\zeta}) - s^2 rw_{,\zeta} w_{,\zeta\eta} \quad (2)$$

$$\begin{aligned} & a_1 I_{,\zeta\zeta\zeta\zeta} + a_2 r^2 I_{,\zeta\zeta\eta\eta} + a_3 r^4 I_{,\eta\eta\eta\eta} + a_4 a^4 I_{,tttt} + a_5 a^2 I_{,\zeta\zeta tt} \\ & + a_6 r^2 a^2 I_{,\eta\eta tt} + a_7 a^2 I_{,\zeta\zeta} + a_8 r^2 a^2 I_{,\eta\eta} + a_9 a^4 I_{,tt} - a^4 I \\ & + a_{10} a^2 (w_{,\zeta\zeta tt} + r^2 w_{,\eta\eta tt}) + a_{11} w_{,\zeta\zeta\zeta\zeta} + a_{12} r^2 w_{,\zeta\zeta\eta\eta} \\ & + a_{13} r^4 w_{,\eta\eta\eta\eta} + a_{14} r^2 w_{,\zeta\zeta\eta\eta tt} + a_{15} w_{,\zeta\zeta\zeta\zeta tt} + a_{16} a^2 w_{,\zeta\zeta tt tt} \\ & + a_{17} r^4 w_{,\eta\eta\eta\eta tt} + a_{18} a^2 r^2 w_{,\eta\eta tt tt} + \frac{a_{19}}{a^2} w_{,\zeta\zeta\zeta\zeta\zeta\zeta} + \frac{a_{20}}{b^2} w_{,\zeta\zeta\zeta\zeta\eta\eta} \\ & + a_{21} \frac{r^4}{a^2} w_{,\eta\eta\eta\eta\zeta\zeta} + a_{22} \frac{r^4}{b^2} w_{,\eta\eta\eta\eta\eta\eta} = 0 \end{aligned} \quad (3)$$

where

$$\begin{aligned} k^2 &= E_\eta/E_\zeta, \quad q^2 = \nu_{\zeta\eta}, \quad p^2 = \mu G_{\zeta\eta}/E_\zeta \\ s^2 &= p^2 + q^2, \quad r = a/b, \quad \mu = 1 - \nu_{\zeta\eta}\nu_{\eta\zeta} \end{aligned}$$

$$\begin{aligned} I &= q(\zeta, \eta) - \rho h w_{,tt} + \frac{N_{\zeta\zeta}}{a^2} w_{,\zeta\zeta} + \frac{N_{\eta\eta}}{b^2} w_{,\eta\eta} + 2 \frac{N_{\zeta\eta}}{ab} w_{,\zeta\eta} \\ \zeta &= x/a, \quad \eta = y/b \end{aligned} \quad (4)$$

In Eqs. (1–4), a comma denotes partial differentiation with respect to the given coordinate. The stress resultants N_{ij} in Eq. (4) are defined in terms of the median surface strains of

the plate as

$$\begin{aligned} N_{\zeta\zeta} &= (E_\zeta h/\mu) (\epsilon_1^0 + q^2 \epsilon_2^0) \\ N_{\eta\eta} &= (E_\zeta h/\mu) (q^2 \epsilon_1^0 + k^2 \epsilon_2^0) \\ N_{\zeta\eta} &= h G_{\zeta\eta} \gamma \end{aligned} \quad (5)$$

where

$$\begin{aligned} \epsilon_1^0 &= \frac{1}{a} u^0_{,\zeta} + \frac{1}{2a^2} w_{,\zeta}^2 \\ \epsilon_2^0 &= \frac{1}{b} v^0_{,\eta} + \frac{1}{2b^2} w_{,\eta}^2 \\ \gamma &= \frac{1}{b} u^0_{,\eta} + \frac{1}{a} v^0_{,\zeta} + \frac{1}{ab} w_{,\zeta} w_{,\eta} \end{aligned} \quad (6)$$

In Eq. (3), the coefficients a_i are functions of orthotropic parameters as well as the tracing constants T_s and R_i , which are used to represent the effect of transverse shear and rotatory inertia, respectively.⁷ For equations applicable to moderately thick plates, these tracing constants should be taken as unity. Similarly, equations corresponding to the classical nonlinear thin-plate theory can be readily obtained by taking the tracing constants as zero. Furthermore, Eqs. (1–3) can be specialized for isotropic plates by taking $k^2 = 1$, $q^2 = \nu$, $p^2 = (1 - \nu)/2$, and $s^2 = (1 + \nu)/2$. In what follows, governing equations (1–3) will be solved for clamped elliptical plates with immovable in-plane edge conditions.

Method of Solution

For a clamped elliptical plate with immovable edges, the conditions to be satisfied along the boundary are

$$w = w_{,\zeta} = w_{,\eta} = u^0 = v^0 = 0 \quad \text{along } 1 - \zeta^2 - \eta^2 = 0 \quad (7)$$

The boundary conditions in terms of w will be satisfied by the following multiple-mode polynomial function:

$$w(\zeta, \eta, \tau) = h(1 - \zeta^2 - \eta^2)^2 [A(\tau) + B(\tau)(1 - \zeta^2 - \eta^2)] \quad (8)$$

where $A(\tau)$ and $B(\tau)$ are known functions of nondimensional time τ , which is defined in terms of t as $\tau^2 = t^2(E_\zeta/\rho a^2)$. Substituting Eq. (8) in Eqs. (1) and (2) and solving for u^0 and v^0 by means of a semi-inverse procedure, it can be shown that

$$\begin{aligned} u^0 &= c_1 \zeta^{11} + c_2 \zeta^9 + c_3 \zeta^7 + c_4 \zeta^5 + c_5 \zeta^3 + c_6 \zeta + c_7 \zeta^9 \eta^2 \\ &+ c_8 \zeta^7 \eta^4 + c_9 \zeta^5 \eta^6 + c_{10} \zeta^3 \eta^8 + c_{11} \zeta \eta^{10} + c_{12} \zeta^7 \eta^2 \\ &+ c_{13} \zeta^5 \eta^4 + c_{14} \zeta^3 \eta^6 + c_{15} \zeta \eta^8 + c_{16} \zeta^5 \eta^2 + c_{17} \zeta^3 \eta^4 \\ &+ c_{18} \zeta \eta^6 + c_{19} \zeta^3 \eta^2 + c_{20} \zeta \eta^4 + c_{21} \zeta \eta^2 \end{aligned} \quad (9)$$

$$\begin{aligned} v^0 &= d_1 \eta^{11} + d_2 \eta^9 + d_3 \eta^7 + d_4 \eta^5 + d_5 \eta^3 + d_6 \eta \\ &+ d_7 \eta^9 \zeta^2 + d_8 \eta^7 \zeta^4 + d_9 \eta^5 \zeta^6 + d_{10} \eta^3 \zeta^8 + d_{11} \eta \zeta^{10} \\ &+ d_{12} \eta^7 \zeta^2 + d_{13} \eta^5 \zeta^4 + d_{14} \eta^3 \zeta^6 + d_{15} \eta \zeta^8 + d_{16} \eta^5 \zeta^2 \\ &+ d_{17} \eta^3 \zeta^4 + d_{18} \eta \zeta^6 + d_{19} \eta^3 \zeta^2 + d_{20} \eta \zeta^4 + d_{21} \eta \zeta^2 \end{aligned} \quad (10)$$

The following procedure is used to determine the 42 coefficients c_i and d_i appearing in Eqs. (9) and (10). The expressions for w , u^0 , and v^0 from Eqs. (8–10) are substituted into Eqs. (1–2). By comparing the coefficients of like terms on both sides of each equation, 30 algebraic equations are generated in terms of c_i and d_i . The in-plane boundary con-

ditions in terms of u^0 and v^0 in Eq. (7) may now be rewritten as

$$u^0 = \int u^0_{,\zeta} d\zeta = \int [e_1(k^2 N_{\zeta\zeta} - q^2 N_{\eta\eta}) - \frac{1}{2} w^2_{,\zeta}] d\zeta = 0 \quad (11)$$

$$v^0 = \int v^0_{,\eta} d\eta = \int [(e_1/r)(N_{\eta\eta} - q^2 N_{\zeta\zeta}) - \frac{1}{2} w^2_{,\eta}] d\eta = 0 \quad (12)$$

where $e_1 = \beta\mu/[E_\zeta(k^2 - q^4)]$ and $\beta = a/h$.

Equation (5) is used to calculate the stress resultants $N_{\zeta\zeta}$ and $N_{\eta\eta}$ from the displacement u^0 and v^0 of Eqs. (9) and (10). Substituting these stress resultants and the expression for w from Eq. (8) in Eqs. (11) and (12), integrations are performed to obtain expressions in terms of c_i and d_i . Comparing the terms of various powers of ζ and η on both sides of these two equations, the 12 algebraic equations can be generated. Thus, for the immovable boundary condition considered here, a total of 42 simultaneous equations are solved to obtain the unknown coefficients c_i and d_i in Eqs. (9) and (10). With these coefficients now fully defined, u^0 and v^0 are completely determined. It must be pointed out here that these are exact solutions to the in-plane displacements u^0 and v^0 . Since this procedure is cumbersome and the coefficients are extremely lengthy, further details are omitted.

Having solved Eqs. (1) and (2) exactly, attention is now turned to the solution of Eq. (3), which represents the dynamic equation of equilibrium in the transverse direction of the vibrating plate. Substituting u^0 and v^0 from Eqs. (9) and (10) and w from Eq. (8) in Eq. (3) and performing the integration over the area of the plate, the following two coupled nonlinear time-differential equations are obtained in terms of the amplitude functions $A(\tau)$ and $B(\tau)$:

$$\begin{aligned} &e_1(A^3)_{,\tau\tau\tau\tau} + e_2(A^2B)_{,\tau\tau\tau\tau} + e_3(AB^2)_{,\tau\tau\tau\tau} + e_4(B^3)_{,\tau\tau\tau\tau} \\ &+ e_5(A)_{,\tau\tau\tau\tau\tau} + e_6(B)_{,\tau\tau\tau\tau\tau} + e_7(A^3)_{,\tau\tau} + e_8(A^2B)_{,\tau\tau} \\ &+ e_9(AB^2)_{,\tau\tau} + e_{10}(B^3)_{,\tau\tau} + e_{11}(A)_{,\tau\tau\tau\tau} + e_{12}(B)_{,\tau\tau\tau\tau} \\ &+ e_{13}A^3 + e_{14}A^2B + e_{15}AB^2 + e_{16}B^3 + e_{17}(A)_{,\tau\tau} \\ &+ e_{18}(B)_{,\tau\tau} + e_{19}A + e_{20}B = q_0^* \end{aligned} \quad (13)$$

$$\begin{aligned} &g_1(A^3)_{,\tau\tau\tau\tau} + g_2(A^2B)_{,\tau\tau\tau\tau} + g_3(AB^2)_{,\tau\tau\tau\tau} + g_4(B^3)_{,\tau\tau\tau\tau} \\ &+ g_5(A)_{,\tau\tau\tau\tau\tau} + g_6(B)_{,\tau\tau\tau\tau\tau} + g_7(A^3)_{,\tau\tau} + g_8(A^2B)_{,\tau\tau} \\ &+ g_9(AB^2)_{,\tau\tau} + g_{10}(B^3)_{,\tau\tau} + g_{11}(A)_{,\tau\tau\tau\tau} + g_{12}(B)_{,\tau\tau\tau\tau} \\ &+ g_{13}A^3 + g_{14}A^2B + g_{15}AB^2 + g_{16}B^3 + g_{17}(A)_{,\tau\tau} \\ &+ g_{18}(B)_{,\tau\tau} + g_{19}A + g_{20}B = q_0^* \end{aligned} \quad (14)$$

Equations (13) and (14) are the modal equations applicable for moderately thick elliptical plates. The nondimensional load q_0^* is equal to $q_0\beta^4/E_\zeta$. The coefficients e_i and g_i in Eqs. (13) and (14) depend upon c_i and d_i given in Eqs. (9) and (10), the orthotropic and material plate parameters, as well as the tracing constants T_s and R_i . When these equations are used for moderately thick plates, the tracing constants are to be taken as unity. However, for equations applicable for thin plates, these constants must be equated to zero. The coefficients e_i and g_i are not explicitly defined in the interest of saving space, but some numerical values for those coefficients are presented later on for the sake of completeness.

For nonlinear static problems concerning moderately thick plates, T_s is equated to unity and R_i is equal to zero. Also, the amplitude functions A and B are independent of time, so that all of the time derivatives in Eqs. (13) and (14) drop out.

Thus, for static problems, these two modal equations reduce to two nonlinear algebraic equations. Solutions to these equations will give the required load deflection relationship. In the case of dynamic problems, Eqs. (13) and (14) can be solved numerically using an IMSL subroutine based on the Runge-Kutta-Verner numerical integration procedure. It must be pointed out here that coefficients e_1 - e_{12} and g_1 - g_{12} depend upon the tracing constants T_s and R_i and, therefore, drop out for thin plates. Such simplified equations are applicable only for thin plates where the effects of transverse shear and rotatory inertia can be ignored. For moderately thick plates, numerical solutions to Eqs. (13) and (14) are obtained with time step size $\Delta\tau = 0.001$ and initial conditions $A(0) = 0, 0.5, 1.0$, and 1.5 ; $A_{,\tau}(0) = 0$; $B(0) = 0$; and $B_{,\tau}(0) = 0$.

Numerical Results and Discussion

Numerical results are presented for static as well as dynamic cases of isotropic and some high-modulus composite elliptical plates. The elastic constants applicable for composite glass/epoxy (GE) and boron/epoxy (BE) plates are taken from Ref. 7. Results for isotropic plates are also presented. In the case of nonlinear static problems, the nondimensional load q_0^* is calculated for various values of the nondimensional central deflection w_0^* , considering simplifications mentioned before for static problems. For each case, a set of nonlinear algebraic equations is solved to obtain the load-deflection values. In the case of dynamic problems, the ratio of the nonlinear frequency ω to the corresponding linear frequency ω_0^* is computed for various nondimensional amplitudes and thickness parameters. The effects of transverse shear and rotatory inertia are included in the calculations of nonlinear frequency, whereas these effects have been omitted for the linear frequency. In some cases, results for thin plates are also presented for the sake of completeness.

The multiple-mode polynomial function in Eq. (8) has been used to compute the linear frequencies for elliptical plates with different aspect ratios. These values are given in Table 1. It is clear that these numerical results are in excellent agreement with those found in the literature.¹¹ In the case of classical thin plates undergoing large deformations, load-deflection values are obtained by dropping the tracing constants and the time-dependent terms from Eqs. (13) and (14) and solving the resulting nonlinear algebraic equations. In Table 2, numerical results are presented for nondimensional load q_0^* at various nondimensional deflection w_0^* , considering the single and multiple terms in the expression for w . Similarly, nondimensional frequency ratios are presented in Table 3 for various values of nondimensional amplitudes for thin plates. Comparisons made in these two

Table 1 Nondimensional frequency parameter
 $\lambda^2 = \omega a^2(\rho/D)^{1/2}$ for elliptical plates

r	Single mode	Multiple mode	Ref. 11
0.5	7.012	6.937	6.937
1.5	17.393	17.206	17.206
2.0	28.048	27.746	27.746

Table 2 Values for nondimensional load q_0^*
for isotropic elliptical plate with $r = 1.5$

w_0^*	Single mode	Multiple mode	Ref. 12
0	0	0	0
0.5	9.29	9.32	9.30
1.0	24.42	26.28	25.10
1.5	51.26	58.31	52.90

Table 3 Values of nondimensional frequency ratio $(\omega/\omega_0) \times 10^4$ for glass/epoxy elliptical plates with $r=1.5$, $T_s=R_i=0$

w_0^*	Single mode	Multiple mode	Ref. 5
0	10000	10000	10000
0.5	10416	10435	10429
1.0	11562	12694	11571
1.5	13236	16412	13247

Table 4 Numerical values of coefficients in Eqs. (13) and (14) for isotropic elliptical plates with $r=2$, $T_s=R_i=1$

Coefficient	e_i	g_i
$\beta=10$:		
1	0.000137	0.000171
2	-0.000386	-0.000503
3	0.000377	0.000509
4	-0.000127	-0.000178
5	0.000406	0.000451
6	-0.000338	-0.000386
7	0.114446	0.142414
8	-0.321594	-0.419630
9	0.313204	0.426175
10	-0.105066	-0.149404
11	0.324206	0.361315
12	-0.270984	-0.311789
13	23.835750	29.457130
14	-66.969280	-87.442790
15	65.206230	89.350550
16	-21.867790	-31.519310
17	64.976660	72.581720
18	-54.435880	-63.115350
19	43.223190	43.223190
20	-37.493630	-56.944670
$\beta=30$:		
1	0.000002	0.000002
2	-0.000005	-0.000006
3	0.000005	0.000006
4	-0.000002	-0.000002
5	0.000045	0.000050
6	-0.000038	-0.000043
7	0.011792	0.014783
8	-0.033275	-0.043382
9	0.032497	0.043893
10	-0.010956	-0.015338
11	0.313366	0.348306
12	-0.261227	-0.298780
13	20.609110	25.810720
14	-58.125650	-75.788840
15	56.746990	76.721860
16	-19.120880	-26.823070
17	544.719700	605.660100
18	-454.241600	-519.952600
19	43.223220	43.223190
20	-32.980740	-52.431730

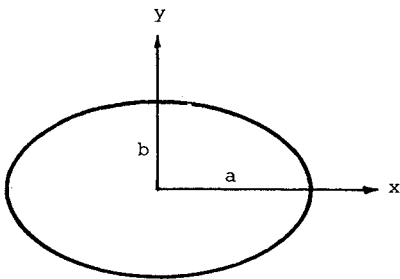


Fig. 1 Geometry and coordinate system.

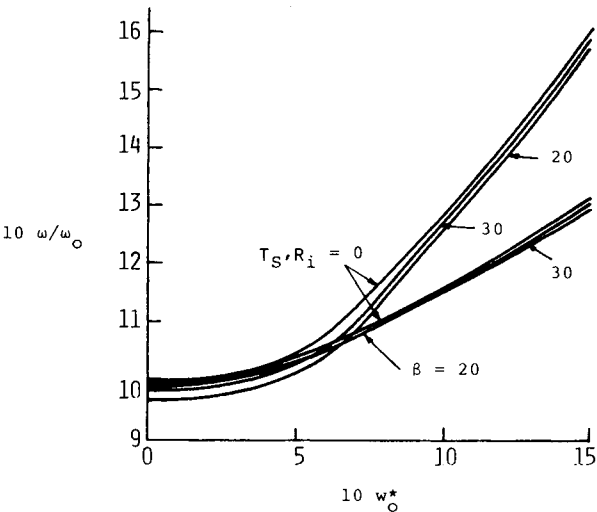


Fig. 2 Variation of frequency ratio with nondimensional amplitude for isotropic elliptical plates with $r=2$.

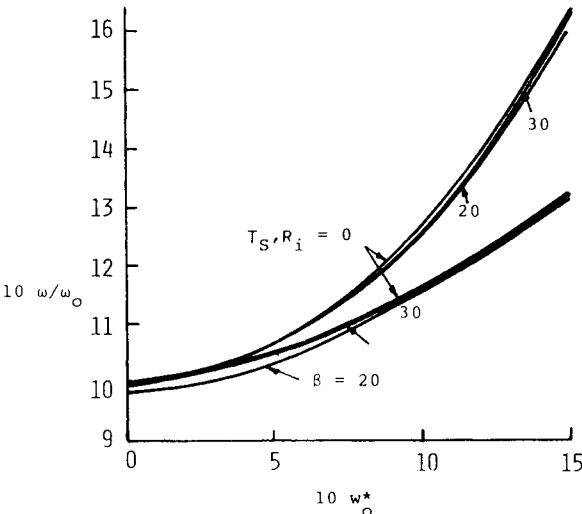


Fig. 3 Frequency ratio vs nondimensional amplitude for glass/epoxy elliptical plates with $r=2$.

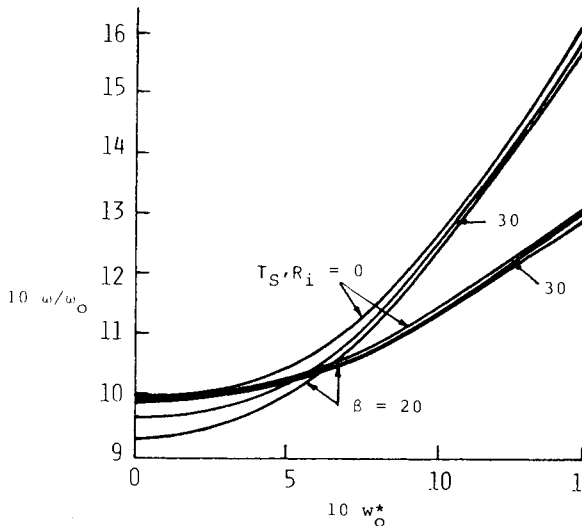


Fig. 4 Variation of frequency ratio with nondimensional amplitude for boron/epoxy elliptical plates with $r=2$.

Table 5 Numerical values of coefficients in Eqs. (13) and (14) for boron/epoxy elliptical plates with $r=2$, $T_s=R_t=1$

Coefficient	e_i	g_i
$\beta = 10$:		
1	0.049009	0.061646
2	-0.138734	-0.181347
3	0.135773	0.183904
4	-0.045995	-0.064458
5	1.101922	1.224363
6	-0.918265	-1.049455
7	2.982468	3.731926
8	-8.351297	-11.085650
9	8.123972	11.343490
10	-2.713010	-4.000415
11	60.621450	67.897590
12	-50.922770	-59.239590
13	39.402700	49.156690
14	-110.401200	-148.429400
15	107.272500	153.705500
16	-35.733100	-54.811900
17	743.175000	835.837400
18	-626.872500	-743.245800
19	56.951900	56.951900
20	-57.288200	-82.917290
$\beta = 30$:		
1	0.000605	0.000761
2	-0.001713	-0.002239
3	0.001676	0.002270
4	-0.000568	-0.000796
5	0.122436	0.136040
6	-0.102029	-0.116606
7	0.276422	0.347454
8	-0.781359	-1.023445
9	0.764071	1.039129
10	-0.258359	-0.364513
11	55.220320	61.416190
12	-46.061750	-52.758170
13	28.032820	35.200790
14	-79.144620	-103.830600
15	77.360970	105.563100
16	-26.109260	-37.062220
17	5531.398000	6157.414000
18	-4618.023000	-5300.570000
19	56.951900	56.951900
20	-44.332670	-69.961540

cases indicate close agreement. A hardening type of nonlinearity is observed in both cases. The results provided by the multiple-mode approach predict higher loads at any given deflection as compared with the results obtained by a single-mode approach. A similar observation can also be made in the case of dynamic problems with respect to the frequency ratios.

In the case of moderately thick plates, Eqs. (13) and (14) have been numerically integrated, using the Runge-Kutta-Verner method, by retaining only those terms whose coefficients are significant. Since the coefficients e_i and g_i are very lengthy to define explicitly, they are tabulated in Tables 4 and 5 for certain chosen parameters of the elliptical plate. Numerical values for the frequency ratios are obtained at

various amplitudes of vibration for certain cases of moderately thick elliptical plates and are graphically presented in Figs. 2-4. For the sake of easy comparison, results corresponding to thin plates are also plotted. Single-mode solutions (SMS) and multiple-mode solutions (MMS) are compared in each figure. For all the cases investigated here, a hardening type of nonlinearity is observed for both moderately thick and thin plates. It is to be noted that there is a significant difference in the numerical values between the single- and multiple-mode solutions. Frequency ratios are lower at any given amplitude when the effects of transverse shear and rotatory inertia are included in the analysis and these effects are found to be predominant at small amplitudes of vibration.

Conclusions

With the aid of von Kármán-type nonlinear equations presented in terms of displacement components of the plate, solutions are presented to the problem of large-amplitude vibration of elliptical plates. Exact solutions are presented to two of the three nonlinear field equations. The effects of transverse shear and rotatory inertia are included conveniently by means of tracing constants and multiple-mode solutions are presented to both nonlinear static and dynamic problems. The effect of modal coupling is found to be significant, at least for all cases reported in this paper.

References

- Chia, C. Y., *Nonlinear Analysis of Plates*, McGraw-Hill, New York, 1980.
- Sathyamoorthy, M., "Nonlinear Vibration of Plates—A Review," *Shock and Vibration Digest*, Vol. 15, 1983, pp. 3-16.
- Herrmann, G., "Influence of Large Amplitudes on Flexural Motions of Elastic Plates," NACA TN-3578, 1955.
- Sathyamoorthy, M., "Nonlinear Vibration of Elliptical Plates," *Journal of Sound and Vibration*, Vol. 70, 1980, pp. 458-460.
- Sathyamoorthy, M. and Chia, C. Y., "Large Amplitude Vibration of Orthotropic Elliptical Plates," *Acta Mechanica*, Vol. 37, 1980, pp. 247-258.
- Banerjee, B., "Large Amplitude Free Vibrations of Elliptical Plates," *Journal of the Physical Society of Japan*, Vol. 23, 1967, pp. 1169-1172.
- Sathyamoorthy, M., "Effects of Large Amplitude, Transverse Shear and Rotatory Inertia on Vibration of Orthotropic Elliptical Plates," *International Journal of Nonlinear Mechanics*, Vol. 16, 1981, pp. 327-335.
- Wu, C. I. and Vinson, J. R., "On the Nonlinear Oscillations of Plates Composed of Composite Materials," *Journal of Composite Materials*, Vol. 3, 1969, pp. 548-561.
- Kanaka Raju, K. and Venkateswara Rao, G., "Axisymmetric Vibrations of Circular Plates Including the Effects of Geometric Nonlinearity, Shear Deformation and Rotatory Inertia," *Journal of Sound and Vibration*, Vol. 47, 1976, pp. 179-184.
- Sathyamoorthy, M. and Chia, C. Y., "Effects of Transverse Shear and Rotatory Inertia on Large Amplitude Vibration of Anisotropic Skew Plates: Part I—Theory," *Transactions of ASME, Journal of Applied Mechanics*, Vol. 47, 1980, pp. 128-132.
- Leissa, A. W., "Vibration of Plates," NASA SP-160, 1969.
- Weil, N. A. and Newmark, N. M., "Large Deflections of Elliptical Plates," *Transactions of ASME, Journal of Applied Mechanics*, Vol. 23, 1956, pp. 21-26.